RAL-93-086

Science and Engineering Research Council

Rutherford Appleton Laboratory

Chilton DIDCOT Oxon OX11 0QX

RAL-93-086

First Results From a Prototype Level-1 Calorimeter Trigger System for LHC

RD 27 (UK) Collaboration

December 1993

FIRST RESULTS FROM A PROTOTYPE LEVEL-1 CALORIMETER TRIGGER SYSTEM FOR LHC

I.P. Brawn, R.E. Carney, J. Garvey, R.J. Staley, A.T. Watson
School of Physics and Space Research, University of Birmingham, Birmingham, UK

E. Eisenhandler, M. Landon
Physics Department, Queen Mary and Westfield College, University of London, London, UK

C.N.P. Gee, A.R. Gillman, R. Hatley, V. Perera
Rutherford Appleton Laboratory, Chilton, Didcot, Oxon., UK

N. Ellis
CERN, Geneva, Switzerland

Presented by A.R. Gillman at the
IV International Conference on Calorimetry in High Energy Physics
La Biodola, Isola d'Elba, Italy
19-25 September 1993

ABSTRACT

As part of the RD27 collaboration, we have studied the problem of level-1 calorimetric triggering and have developed an algorithm to identify electromagnetic energy clusters. This algorithm has been incorporated into a prototype CMOS Application-Specific Integrated Circuit (ASIC) running as a pipelined processor at up to 67 MHz. In order to verify the operation of the processor in a realistic environment, a multi-ASIC demonstrator system has been constructed and used to instrument small regions of two prototype electromagnetic calorimeters in CERN test beams.

We present here details of the demonstrator system and analysis of the data which have been taken so far. The results show that the demonstrator system performs successfully and recognises electromagnetic clusters efficiently at LHC rates.

To realise a complete level-1 trigger system several further areas require study. In particular, data bandwidth must be minimised by using sparsification techniques, and I/O requirements reduced by serialisation. These approaches imply the use of asynchronous systems, the features of which we intend to study in the next phase of this work.

1. Introduction

At the LHC design luminosity, the proton–proton interaction rate will be ~10^9 Hz with a bunch-crossing rate of 40 MHz, presenting very challenging conditions for triggering at level-1. With a typical readout time of 10 μs for subdetectors, the rate into the level-2 trigger system must not exceed 100 kHz, thereby requiring a rejection of ~10^4 from the level-1 trigger. High trigger efficiency is demanded by the very small cross-sections of many of the interesting physics processes, and the trigger system should be as flexible as possible to adapt to new physics or unforeseen background conditions.

In RD27[1,2] we have been investigating a custom-built, synchronous digital processor for a level-1 calorimeter trigger, based on Application-Specific Integrated Circuits (ASICs). A digital approach has numerous advantages, e.g. easy implementation of complex algorithms with programmable parameters, and provision for calibration, monitoring and diagnostics. ASIC technologies adequate for our needs are already available, and we can exploit future developments in this area to add functionality and/or reduce system cost.

2. Simulation studies

In order to achieve the required rejection ratio of ~10^4, while maintaining high efficiency for interesting physics processes, the level-1 trigger system must operate with carefully-chosen criteria. Several different trigger algorithms have therefore been studied by simulating the response of a typical LHC detector to possible LHC events[3].

2.1. Algorithms

The electron/photon trigger is based on a localised deposit of transverse energy (E_T) in the electromagnetic calorimeter. Ideally, this cluster should fully contain the energy of an e.m. shower whilst being small in comparison with a jet core.

Our simulation work suggests that a reduced detector granularity of $\Delta\eta \times \Delta\phi \approx 0.1 \times 0.1$ (with one depth sampling in each of the electromagnetic and hadronic calorimeters — ECAL and HCAL) is acceptable, so this has been used in all the algorithms studied. By allowing only the cells above a certain E_T threshold to contribute to the trigger, sensitivity to electronic noise and pileup is reduced.

The important parameters for an electromagnetic cluster algorithm are trigger threshold sharpness and background trigger rate. Threshold sharpness is affected by the degree of containment of e.m. showers within the cluster window, the resolution of the calorimeter and digitisation system and by electronic noise and pileup, whereas the background rate (dominated by hadronic jets) is determined primarily by the area of the cluster window. As many of the interesting physics processes result in *isolated* leptons or photons, a further trigger rate reduction can be achieved using isolation requirements.

We have calculated efficiencies for three different cluster definitions (1×1, 2×1 and 2×2 cell E_T clusters above threshold) for 50 GeV electrons at $|\eta| \approx 0$. The 1-cell algorithm exhibits a significantly softer threshold than the 2-cell and 4-cell algorithms due to shower leakage at the cell edges. For this granularity, the 2-cell algorithm exhibits a threshold almost as sharp as that of the 4-cell one, but the much lower trigger rate it produces makes it our preferred algorithm; it is shown schematically in Figure 1.

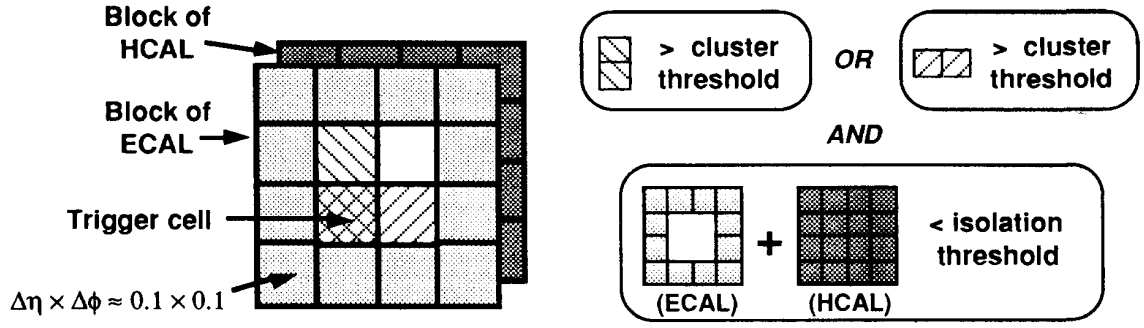

Figure 1: Cluster algorithm.

Further jet rejection can be obtained by forming the E_T sums in a ring of e.m. cells surrounding the cluster, and in the hadronic window behind it. The effectiveness of the isolation cuts is determined by the area of the isolation window and by the tightness of the cuts which can be applied whilst still retaining high efficiency for isolated e.m. showers. The cuts are limited by electronic noise, pileup and leakage of the shower itself into the isolation regions. Application of an E_T threshold to the individual trigger cells suppresses electronic noise and pileup but also reduces the sensitivity to low-p_T jet fragments and hence the effectiveness of the isolation requirement, so this threshold value is crucial to the performance of the isolation veto. A threshold of 1 GeV per trigger cell was generally used.

2.2 Estimated trigger rates

We have estimated trigger rates for the most difficult case, where the peak LHC luminosity is taken as 1.7×10^{34} cm^{-2}s^{-1}. We aim for an inclusive e.m. cluster threshold of $\approx$ 40 GeV and a trigger on pairs of clusters with thresholds of $\approx$ 20 GeV. The e.m. cluster trigger rates

obtained are shown in Figure 2 for single-cluster and two-cluster triggers, with and without isolation requirements. Note that the isolation requirement reduces the background rate by an order of magnitude at the desired thresholds.

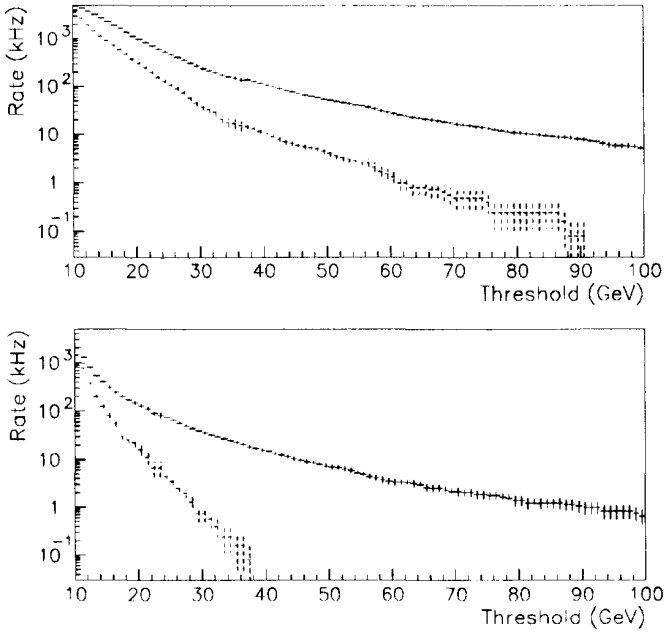

Figure 2: Trigger rate vs threshold at $L = 1.7 \times 10^{34}$ $cm^{-2}s^{-1}$, without isolation (upper curves) and with isolation (lower curves): (a) Single e.m. cluster rates, (b) Two e.m. cluster rates.

3. Demonstrator system

We have designed, constructed and tested a first-prototype calorimeter trigger system[4,5]. Its aim was to verify the efficiency and rejection power of the selected e.m. cluster-finding algorithm, running at full LHC speed and using affordable present-day electronics, with real-time signals from prototype LHC calorimeters in a test-beam environment. The core of this system is an ASIC that implements most of the features of our trigger algorithm[6].

3.1. Description of the ASIC

The ASIC carries out the operations needed by the algorithm for one e.m. trigger channel (hadronic data are not processed in this first prototype chip), using 8-bit energy values from 16 trigger cells. Separate energy sums are formed with one horizontal and one vertical neighbour to find potential e.m. clusters, and the energy in the outer 12 e.m. cells is summed to examine isolation. As shown in Figure 1, a cluster is found if the vertical or the horizontal sum is greater than a programmable cluster threshold, and the sum of the outer 12 cells is less than a programmable isolation threshold. This logic is duplicated, with two pairs of programmable threshold values to allow for two different cluster conditions. The energy sum of all 16 input cells is also formed, for use in future jet and missing-E_T logic.

The ASIC is a 0.8 μm CMOS gate array from Fujitsu, packaged as a 179-pin ceramic pin-grid array. The algorithm is implemented as a sequence of pipelined arithmetic stages, with the 12-bit total energy sum emerging after a latency of 6 clock cycles, and the cluster-found flags after 7 clock cycles. Tests up to 70 MHz have been successful.

3.2. Prototype calorimeter trigger processor system

Our current trigger system (Figure 3) uses nine ASICs to fully process a 3×3 area of calorimeter trigger cells, for which the algorithm demands data from a 6×6 area. Signals are

first digitised in three 12-channel 8-bit flash-ADC (FADC) modules and then passed to a cluster-finding module (CFM) containing the nine ASICs.

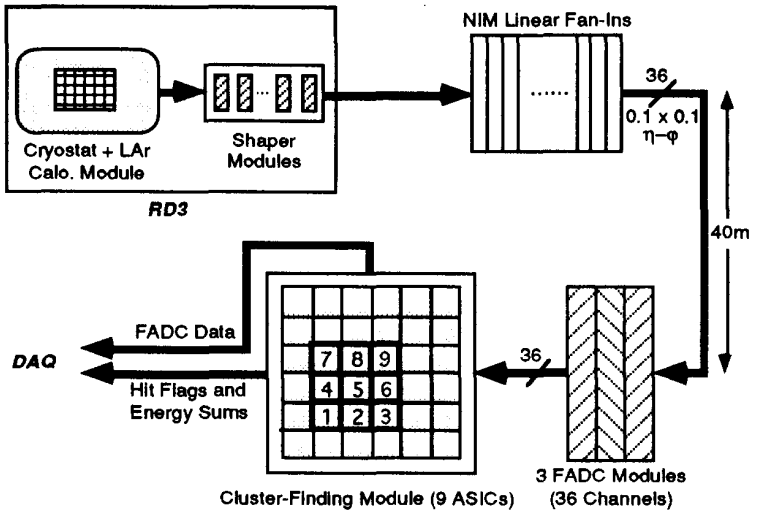

Figure 3: Block diagram of the calorimeter and trigger system.

All modules are 9U high and 40 cm deep and utilise two backplanes. The upper wire-wrap backplane, using Teradyne connectors with 320 active pins and 80 grounds, permits flexible high-speed (ECL) data and clock interconnections between modules, while the lower one provides a simple control/addressing system interfaced to VMEbus.

Synchronisation of modules within the trigger crate is under the control of a clock module, which distributes correctly-phased strobe signals to the three FADC modules and to the CFM. During each system clock cycle, digital data from the 36 FADC channels are transferred in parallel to the CFM and injected into a pipeline running at the system clock frequency. Trigger bits resulting from the trigger cluster-finding algorithm emerge seven clock cycles later from the ASICs and are available as prompt front-panel outputs.

Copies of the incoming FADC information, output trigger hits and ASIC energy sums are stored in the CFM in high-speed memories, allowing up to 256 time slices to be recorded. During operation the system clock free-runs and the memories scroll continuously at the system clock frequency, so at any instant the memories contain a history of the preceding 256 FADC samples and the corresponding trigger algorithm results from the nine ASICs.

On receipt of an event signal, the clock module counts a further programmable number of system clock cycles before generating a stop signal to freeze the CFM memories. The event signal is also sent to a VME-based data acquisition system, which selectively reads out and records the CFM memory contents, and performs on-line analysis on a sample of the data.

3.3. Beam tests

We recorded data in CERN test beams both with the RD3 prototype liquid-argon Accordion calorimeter[7] and with the RD33 prototype TGT liquid argon calorimeter[8]. As the analysis of the latter is still in progress, the following relates solely to the RD3 tests[9].

To form trigger cells of the desired granularity, analogue signals from the calorimeter were added both laterally and in two $9X_0$ depth samples (Figure 3). A system-clock frequency of 40 MHz, corresponding to the 25 ns LHC bunch-crossing period, was used for most data collection although some data were also taken at the original design frequency of 67 MHz. Using beam positions near the centres, edges and corners of trigger cells we recorded data with different combinations of beam energy and particle type, and with several different cluster and isolation thresholds in the trigger. Most of the running time was devoted to an extensive position scan of the calorimeter using 300 GeV electrons.

We calibrated the FADCs with electron beam data of several energies, measuring a sensitivity close to our design goal of 1 GeV/count. Digitisations prior to the arrival of the

pulse gave pedestal values and rms widths of typically 26 GeV and 0.6 GeV respectively. The observation of low rms values is important because the noise levels seen in unoccupied channels have a considerable impact on the performance of the trigger, especially in the isolation veto.

Since the trigger clock period is short compared with the Accordion calorimeter pulse, the signal from a single shower is typically sampled over several 40 MHz clock cycles, as shown in Figure 4. For a pipelined level-1 trigger processor, only the sampling corresponding to the peak of the analogue pulse should enter into the evaluation of the cluster-finding algorithm for a particular crossing. All other samplings must be set to zero or they will contribute to triggers associated with earlier or later crossings.

We are therefore exploring techniques for bunch-crossing identification (BCID), using digital signal-processing algorithms which we have simulated in software and exercised with our test-beam data. Peak-finding algorithms, for example, have already yielded very encouraging results, even for relatively small deposited energies[10].

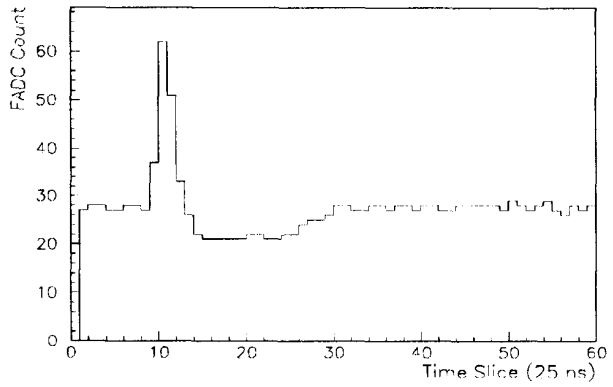

Figure 4: Accordion calorimeter pulse sampled at 40 MHz.

To study the trigger threshold sharpness the electrons must be evenly distributed over the trigger acceptance, so in a test-beam environment one needs a number of data samples taken over a range of points within a trigger cell. Our beam spot was about the size of a single calorimeter cell and a trigger cell was the sum of 4×4 calorimeter cells, so a representative distribution was obtained by combining data from 50 GeV electrons seen in the 4-cell core (1 run), in a corner (1 run) and along an edge (2 runs).

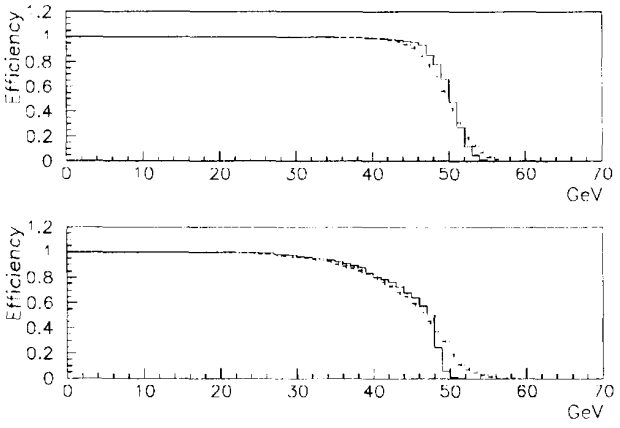

Figure 5: Efficiency vs threshold (solid lines = test-beam, dashed lines = Monte Carlo): (a) for two-cell algorithm, (b) for single-cell algorithm.

Figure 5(a) shows the efficiency of the cluster algorithm computed as a function of threshold, together with the Monte Carlo expectation for a similar calorimeter geometry. Figure 5(b) shows the much softer threshold behaviour for a trigger based on a single cell. In both cases simulation and data agree well.

Recording both the FADC data and the ASIC outputs enabled us to compare the energy sum calculation of the ASIC-embedded algorithm with its software counterpart. 80% of events show perfect correlation, and in the remaining events exact agreement is still found, but a trivial memory timing error (now corrected) had produced a timing slip. Figure 6 shows the correlation after correcting for this readout problem in the analysis.

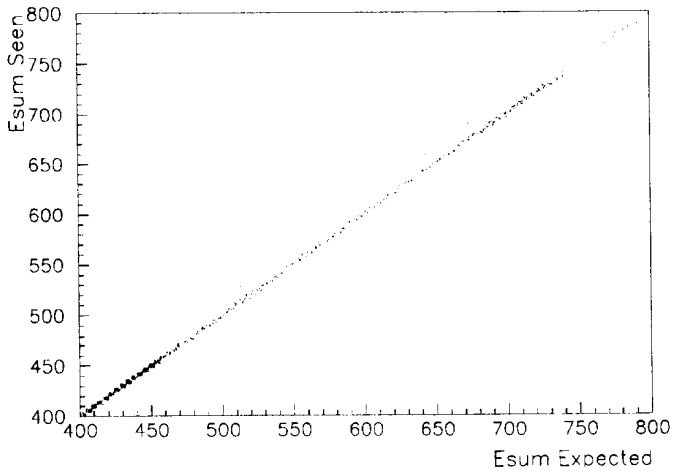

Figure 6: ASIC energy-sum output vs expected value.

To study the two types of thresholding operations separately, the isolation requirement was disabled in some data-taking runs. Figure 7 shows the effect of the cluster threshold set just above the pedestal sum for two channels, and Figure 8 shows the effect of the isolation threshold set close to the expected 12-channel pedestal sum. Choosing events in which one of the clusters should be above the cluster threshold, one can compare the isolation sums in events for which the trigger hit was or was not present.

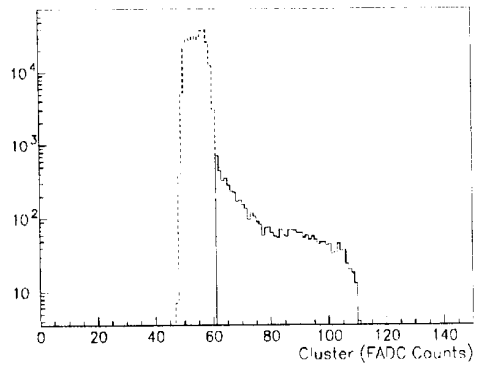

Figure 7: Energy in cluster window for events with (solid line) and without (dashed line) a trigger hit.

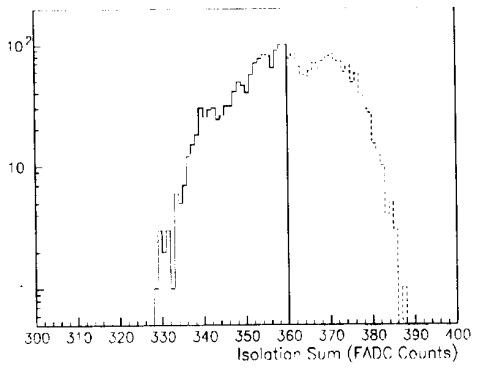

Figure 8: Energy in isolation window for events with (solid line) and without (dashed line) a trigger hit.

The ability of the trigger processor to separate electrons from pions and muons in real time was demonstrated by examining the RD3 data tapes. Figure 9(a) shows the energies observed in the RD3 e.m. and hadronic calorimeters plotted against each other and Figure 9(b) shows

the same distribution for events in which the RD27 e.m. cluster trigger fired. The effective trigger threshold was approximately 150 GeV.

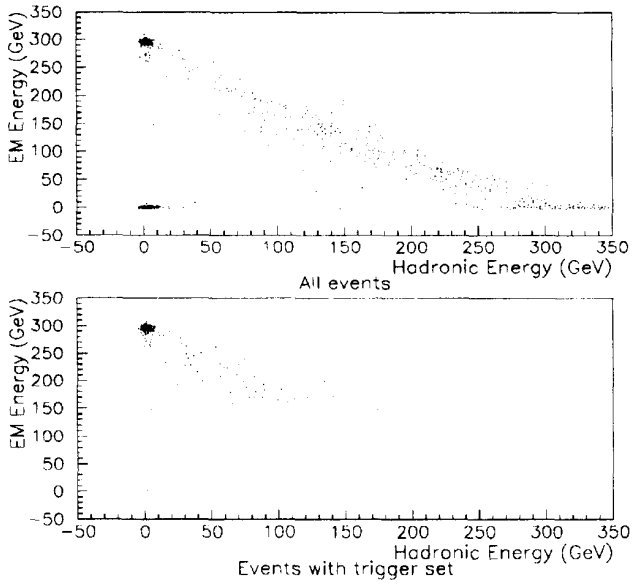

Figure 9: Energy in ECAL vs energy in HCAL:
(a) for all events, (b) for events with e.m. cluster trigger hit.

Three distinct event types can be seen – events with a large deposit of energy in the e.m. calorimeter and none in the hadronic calorimeter (electrons), events with little or no energy in either calorimeter (muons), and events in which energy is shared between the two calorimeters (pions).

Another important test of the trigger algorithm is its ability to distinguish electrons from pions. Cluster and isolation thresholds were chosen to achieve a high efficiency (> 95%) for electrons with energies of 10, 20 and 30 GeV, and these were then applied to pion data. A substantial rejection (*e.g.* ~42 at 20 GeV) is obtained from the cluster threshold alone, with the e.m. isolation requirement contributing little further, as expected for single particles. Hadronic isolation would improve this significantly.

4. Future work

With nine ASICs, the current CFM fully processes a 3 × 3 area of ECAL trigger cells, so a full-scale ECAL (with ~4000 trigger channels) would demand several hundred such modules. Techniques must therefore be found to raise the number of trigger channels processed by each trigger module. Simply increasing the number of trigger channels processed per ASIC rapidly leads to I/O bottlenecks both at the ASIC and module level. For example, an ASIC built to process a 4 × 4 trigger cell array from both ECAL and HCAL would require over 800 I/O pins alone, and a CFM containing only 4 such ASICs would need ~2000 I/O backplane connections, which is clearly not feasible.

Various techniques have been explored to address these problems, particularly that of large bandwidth demands. A possible solution has been found, based on data sparsification and high-speed serialisation techniques, which has as its core a 0.5 μm CMOS ASIC fully processing 16 trigger cells. This ASIC would receive 98 serial bit-streams of asynchronous zero-suppressed data from a 7 × 7 area of ECAL and HCAL, each at 160 Mbit/s, and would provide eight sets of programmable threshold values. Mounting four such ASICs on a cluster processing module would enable a full level-1 calorimeter trigger processor to be designed and constructed using only six crates[11].

We have identified several key areas of this system that require further study before such a processor could be constructed. A phase-2 trigger demonstrator system will therefore be built

to test the full data sparsification scheme, comprising zero-suppression and asynchronous serial data transfer optically at 160 Mbit/s. BCID will be implemented in hardware and we will study the associated tagging/matching function.

This system will require the design of a new high-speed dual-mode ASIC, whose function will be to operate explicitly as a test bench and allow an evaluation of the proposed solution. To process a 3×3 area of the calorimeter, several of these ASICs will be incorporated in a new demonstrator system which ultimately will be tested on calorimeter data in a test-beam environment.

Acknowledgements

We gratefully acknowledge the considerable help we received from RD3, both in allowing us to use signals from their calorimeter and in performing the beam tests.

References

1. RD27 proposal, CERN/DRDC/92–17.
2. RD27 status report, CERN/DRDC/93-32.
3. A. Watson, Physics Simulation Studies of the First-Level Electron/Photon Trigger, *RD27 note 13* (1993).
4. N. Ellis et al., A calorimeter-based level-one electromagnetic cluster trigger for LHC, *Proc. CHEP92*, CERN 92–07 pp 210–213.
5. E. Eisenhandler et al., First-level calorimeter trigger system for the LHC, *Proc. IEEE Nuclear Science Symposium* (1992).
6. V. Perera, Data on the LHC electromagnetic cluster-finding ASIC (RAL 114), *RAL* (1992).
7. RD3 proposal, CERN/DRDC/90–31.
8. RD33 proposal, CERN/DRDC/93–2.
9. R.E. Carney et al., The Level-1 Bit-Parallel Electromagnetic Trigger Processor. CERN Beam Tests—November 1992, *RD27 note 12* (1993).
10. I. Brawn, Preliminary investigations into bunch-crossing identification for the level-1 trigger, *RD27 note 11* (1993).
11. V. Perera, A First-Level Calorimeter Trigger Processor for the Large Hadron Collider, *RD27 note 8* (1993).